# Singular values behaviour optimization in the diagnosis of feed misalignments in radioastronomical reflectors

Capozzoli, Amedeo, Curcio, Claudio, Liseno, Angelo, Savarese, Salvatore, Schipani, Pietro

Amedeo Capozzoli, Claudio Curcio, Angelo Liseno, Salvatore Savarese, Pietro Schipani, "Singular values behaviour optimization in the diagnosis of feed misalignments in radioastronomical reflectors," Proc. SPIE 9912, Advances in Optical and Mechanical Technologies for Telescopes and Instrumentation II, 99124P (22 July 2016); doi: 10.1117/12.2233403

SPIE.

Event: SPIE Astronomical Telescopes + Instrumentation, 2016, Edinburgh, United Kingdom

# Singular values behaviour optimization in the diagnosis of feed misalignments in radioastronomical reflectors

Amedeo Capozzoli[*a], Claudio Curcio[a],
Angelo Liseno[a], Salvatore Savarese[a], Pietro Schipani[b]
[a]Università degli Studi di Napoli Federico II - Dipartimento di Ingegneria Elettrica e Tecnologie dell'Informazione (DIETI), via Claudio 21, 80125 Napoli (Italy);
[b]INAF - Istituto Nazionale di Astrofisica - Osservatorio Astronomico di Capodimonte - Salita Moiariello, 16 - 80131 Napoli (Italy)

## ABSTRACT

The communication presents an innovative method for the diagnosis of reflector antennas in radio astronomical applications. The approach is based on the optimization of the number and the distribution of the far field sampling points exploited to retrieve the antenna status in terms of feed misalignments, this to drastically reduce the time length of the measurement process and minimize the effects of variable environmental conditions and simplifying the tracking process of the source. The feed misplacement is modeled in terms of an aberration function of the aperture field. The relationship between the unknowns and the far field pattern samples is linearized thanks to a Principal Component Analysis. The number and the positon of the field samples are then determined by optimizing the Singular Values behaviour of the relevant operator.

**Keywords:** Antenna Diagnosis, Radiotelescopes, Microwave Holography, Far Field Measurements, Antenna Measurements, Singular Value Decomposition, Sampling Methods, Microwave Measurements

## 1. INTRODUCTION

In order to get the best performances of large reflector antennas for radio astronomical applications, a continuous monitoring and the reassessment of the Antenna Under Test (AUT) is necessary [1-3]. In particular, getting the maximum gain and the correct pointing angle require the suppression of the deviations of the reflecting surfaces [4] from their nominal profiles, and the correct alignment of reflectors and feeding structure.

Among the different approaches adopted in the last decades, the electromagnetic monitoring appears today one of the most appealing. The electromagnetic monitoring allows in-situ measurements, with little direct human intervention, and employs a relatively simple setup. The approach retrieves the distortions and the misalignments from amplitude and phase, or only amplitude, measurements of Far-Field Pattern (FFP) of the AUT. The FFP is typically measured with the AUT in the receiving mode and by adopting a natural radio star or a satellite beacon as the signal source [1,2]. To acquire the FFP in amplitude and phase, a second antenna must be considered to generate a reference signal, allowing the holographic approach [4]. A simpler approach is possible by measuring the amplitude of the FFP only [5-7]. This alternative does not require any reference antenna and demands a simpler measurement setup. Obviously, additional information about the AUT or a second set of measurements is required to restore the missed information.

In both cases, a very large number of field samples is required to get the complete information about the AUT, making the measurement process lengthy. On the other hand the acquisition process is burdened due to difficulties of a continuous tracking of the source and inconstancy of the environmental conditions.

A proper strategy turns relevant, to reduce as much as possible the time length of the measurements process, and to increase the robustness of the inversion against noise and reduced dynamical ranges.

Indeed it is expected that the number of parameters to be retrieved on the AUT significantly influences the acquisition strategy.

[*]Send correspondence to A. Capozzoli: a.capozzoli@unina.it

Advances in Optical and Mechanical Technologies for Telescopes and Instrumentation II, edited by Ramón Navarro, James H. Burge, Proc. of SPIE Vol. 9912, 99124P

In particular, as long as only low order aberrations must be evaluated, a smaller set of data is needed. This is the case of a "reduced" diagnosis of feed and sub-reflector (if present) misalignments, or of a "full" diagnosis involving also the distortions of the primary reflector surface [8].

Aim of the paper is to present an approach to define the number and the distribution of the FFP samples according to the desired monitoring resolution. The approach recasts the diagnosis in terms of a linear inverse problem, and the goal is achieved thanks to a Singular Values Behavior (SVB) optimization of the relevant operator mapping the parameters defining the misalignments to the FFP.

The paper is organized as follows. Section 2 introduce the mathematical model of the problem, in Section 3 the solution algorithm is presented, while Section 4 shows and discusses some numerical results limited to the case of a lateral feed displacement. The performances are compared to those of a standard approach based on a standard sampling acquisition scheme.

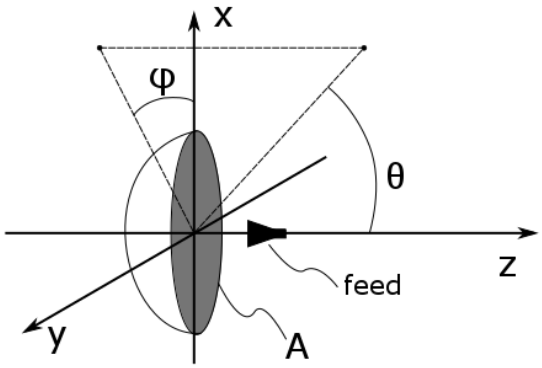


Figure 1. Geometry of the problem.

## 2. STATEMENT OF THE PROBLEM

Let us consider as AUT a reflector antenna, whose aperture A lies in the z=0 plane of the (Oxyz) reference system schematically depicted in Figure 1.

The Aperture Field (AF) method is employed to describe the radiation mechanism of the AUT. In particular, for the sake of simplicity and without any loss of generality, we consider a scalar problem, assuming that the AF, say $\underline{E}_a$, is linearly polarized along the x-axis: $\underline{E}_a = E_a \underline{i}_x$. Monochromatic signals will be considered, and the time dependence $exp(j\omega t)$ assumed and dropped.

The relationship between the x-component of the FFP, say F, and $E_a$ is easily expressed, apart from inessential constants, via the well-known Fourier Transform relationship [9]:

$$F(u,v) = \sqrt{1-u^2-v^2} \iint_A dx\, dy\, E_a(x,y) exp\big(j\beta(ux+vy)\big) = \mathcal{T}\,[E_a] \qquad (1)$$

where:

- $u = \sin\theta\cos\varphi$ and $v = \sin\theta\sin\varphi$ are the cosine directors, $(\theta,\varphi)$ being the spherical angles depicted in Figure 1;
- $\beta = 2\pi/\lambda$, $\lambda$ being the wavelength;
- $\mathcal{T}$ is the operator mapping the AF on the FFP.

Misalignments and distortions of the reflecting surfaces alter $E_a$ from its nominal value. Accordingly, monitoring the AUT amounts at determining first $E_a$ from the FFP, and then inverting the desired configuration parameters.

In the paper we focus our attention on the misalignment of the feeding system. Assuming that its displacement keeps small, we can assume that the deviation from the nominal configuration affects only the phase distribution of $E_a$. We can

then introduce a real valued aberration function $\Phi(x, y; p_1, \dots, p_N)$ representing the phase perturbation as a function of N parameters $p_1, \dots, p_N$ describing the status of the AUT to be retrieved. With these assumptions, the AF can be written as:

$$E_a(x, y) = E_{a0}(x, y) exp\big(j\Phi(x, y; p_1, \dots, p_N)\big) \tag{2}$$

where $E_{a0}$ is the nominal AF, corresponding to the undistorted configuration.

The diagnosis problem consists of determining $\Phi$ from the FFP, and then the parameters $p_1, \dots, p_N$ describing its status. Accordingly, the solution of an inverse problem is required.

## 3. THE SOLUTION ALGORITHM

To recast the inverse problem as a linear one, we consider a proper representation of $exp\big(j\Phi(x, y; p_1, \dots, p_N)\big)$, noting that it defines a manifold $\mathcal{M}$ in the space of functions with two variables $(x, y)$, as long as $(p_1, \dots, p_N)$ are varied in the intervals defining the acceptable indeterminacies for the parameters defining the AUT status. We can then introduce the set of basis functions $\{\psi_1, \dots, \psi_K\}$ defining the smallest subspace containing $\mathcal{M}$. Accordingly:

$$exp\big(\phi(x, y; p_1, \dots, p_N)\big) = \sum_{k=1}^{K} c_k(p_1, \dots, p_N)\psi_k(x, y) \tag{3}$$

The set of basis functions $\{\psi_1, \dots, \psi_K\}$ can been found thanks to a Principal Component Analysis (PCA).

Concerning the FFP, it is assumed sampled at S points $(u_s, v_s)$. Equation (1) can be then written in matrix form as:

$$\underline{F} = \underline{\underline{T}}\,\underline{C} \tag{4}$$

where $\underline{F}$ and $\underline{C}$ are the S-dimensional vector containing the field samples and the K-dimensional vector of the expansion coefficients, respectively. The entries of the matrix $\underline{\underline{T}}$ are given by:

$$T_{sk} = \langle \mathcal{T}\,[E_{a0}\psi_k], \delta(u - u_s)\delta(v - v_s)\rangle \tag{5}$$

$\delta$ being the Dirac distribution.

Retrieving the AUT status amounts at finding the coefficients $c_k$, and then the parameters $p_1, \dots, p_N$, from $\underline{F}(u_s, v_s)$. As a consequence, the inversion of the linear algebraic system in Equation (4) is required. Obviously, such a system can suffer from the ill-conditioning, with detrimental effects on the accuracy of the reconstruction and on the robustness against noise.

$\underline{\underline{T}}$ depends on the samples distribution in the $(u, v)$ plane. We consider a plane-polar arrangement of $(u_s, v_s)$, so that they are located on M rings with radii $\rho_m$, and therein uniformly spaced with sampling step $\Delta\chi_m$ [8,10].

Before inverting $\underline{\underline{T}}$, the most convenient matrix must be picked up, by optimizing its SVB as a function of M, $\rho_m$ and $\Delta\chi_m$.

The optimization of the SVB of $\underline{\underline{T}}$ can be obtained by maximizing the functional [11]:

$$\Psi\left(\underline{\rho}, \underline{\Delta\chi}\right) = \sum_r \frac{\sigma_r\left(\underline{\rho}, \underline{\Delta\chi}\right)}{\sigma_1\left(\underline{\rho}, \underline{\Delta\chi}\right)} \tag{6}$$

where $\underline{\rho}$ and $\underline{\Delta\chi}$ are the M-dimensional vectors containing the radii $\rho_m$ and the sampling steps $\Delta\chi_m$, respectively, and $\sigma_r$ are the Singular Values of $\underline{\underline{T}}$, arranged in a decreasing order.

The Global Optimization of $\Psi$ is obtained using a Differential Evolution approach [12].

### 3.1 Feed Position Retrieval

Once the aberration function is obtained, the feed position is retrieved through a second optimization procedure. Considering a feed displacement from the nominal position $(\Delta x, \Delta y, \Delta z)$, as shown in Figure 2, the aberration function

can be obtained by applying Geometrical Optics (GO). Since we are interested only in the phase perturbation of $E_a$, the solution of the transport equation is not required, and only the optical path from the feed to the aperture through the reflection must be calculated. In principle, an approach like [13] could be used, but a standard Ray-Tracing algorithm, particularly if optimized [14], is much more efficient, being the medium wherein the AUT is embedded homogeneous. Therefore the displacement $(\Delta x, \Delta y, \Delta z)$ can be found minimizing the functional:

$$\Psi_{GO} = \left\| E_{a0} exp\left(j\Phi_{GO}(x, y, \Delta x, \Delta y, \Delta z)\right) - E_{a0} exp\left(j\phi(x, y)\right) \right\| \quad (7)$$

Where $\Phi_{GO}$ is the phase distorsion calculated thanks to GO, as a function of the feed position.

This second optimization step can be straightforwardly obtained by using a gradient-based Local Optimizer.

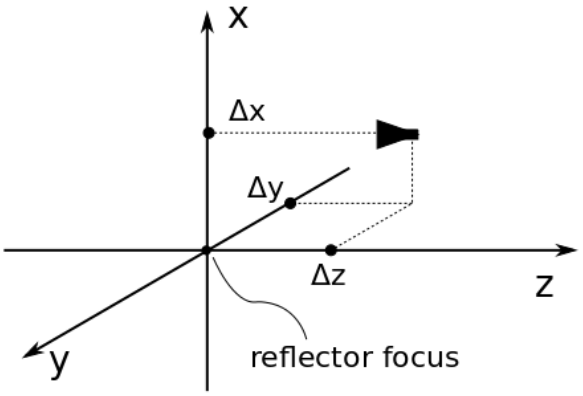


Figure 2. Geometry of the feed displacement.

## 4. NUMERICAL RESULTS

In this section some results of a wide numerical analysis are presented. Here we consider a lateral displacement translating a linear aberration, but the procedure can be nonetheless extended to include higher order aberrations. To assess the performances, we compare the results with those obtained using a standard approach, based on a standard uniform Cartesian sampling grid, whose spacing agrees with the Nyquist sampling criterion.

In the worked example, the AUT is a centered parabolic reflector working at 10GHz. The diameter of the reflector and its focal length are equal to 0.85m (~28λ) and 0.5m, respectively. The field radiated by the feed is linearly polarized, with an asymmetric tapering along the x-axis and the y-axis of $-12dB$ and $-16dB$, respectively. To realistically simulate the field radiated by the AUT, we used the PO solver the commercial software FEKO has been used. The amplitude of $E_{a0}$ is shown in Figure 3. The introduced misalignment is summarized Table 2.

To represent the effects of the lateral displacement of the feed on $E_a$, the aberration function has been expressed as:

$$\Phi = p_1 \mathrm{x} + p_2 \mathrm{y} \quad (8)$$

To calculate the PCA, a discretization of $\mathcal{M}$ has been considered by varying the parameters $p_1, p_2$ in the range $[-5,5] \times [-5,5]$, related to a maximum displacement of 50mm. Thanks to the PCA, an accurate representation of Φ can be obtained by using 19 basis functions.

To make a realistic example, the far-field data has been corrupted by an additive white Gaussian noise with a signal to noise ratio of 30dB. Figure 4 presents the amplitude of the FFP to be sampled.

After the optimization of the SVB of $\underline{\underline{T}}$ a sampling grid of 24 points distributed over 2 rings appears sufficient to make the diagnosis possible. The values of ρ and Δχ are summarized in Table 1.

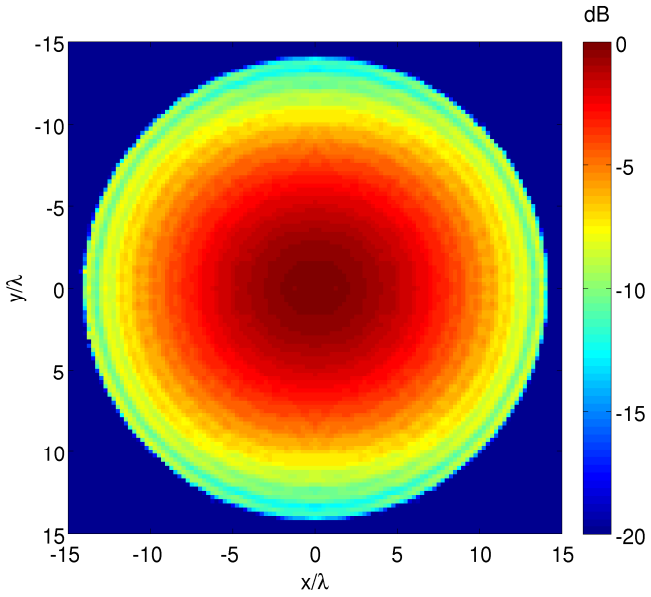


Figure 3. Normalized amplitude in dB of the nominal aperture field $\boldsymbol{E_{a0}}$.

For the sake of comparison a standard approach has been implemented. Only the region $[-0.3,0.3] \times [-0.3,0.3]$ of the $(u, v)$ plane has been taken into account, to avoid measurements of useless FFP samples significantly corrupted by the noise. For this second case, the overall number of sampling points is equal to 361, significantly larger than that of the proposed approach. Figure 5 shows the SVB for both cases.

Table 1. Parameters of the Optimized sampling grid.

| **Rings** | **ρ** | **Δχ** |
|---|---|---|
| **1** | 0.0442 | 0.5218 |
| **2** | 0.0707 | 0.5209 |

The amplitude of the reconstructed FFP is displayed in Figure 6 while Figure 7 displays a cut along the u-axis, showing that both grids can effectively represent the FFP of the AUT.
Figure 8 shows the Φ retrieved in both cases. The displacement of the feed from the reflector focus corresponding to the retrieved Φ is compared to its nominal position in Table 2, showing an error of 0.15mm ($\sim 5 \cdot 10^{-4}\lambda$) in the diagnosis of the position.

Table 2. Displacement of the feed.

| | **Δx [mm]** | **Δy [mm]** | **Δz [mm]** |
|---|---|---|---|
| **Nominal** | 5.0 | 7.0 | 0.0 |
| **Retrieved** | 5.13 | 7.05 | $2.1 \cdot 10^{-2}$ |

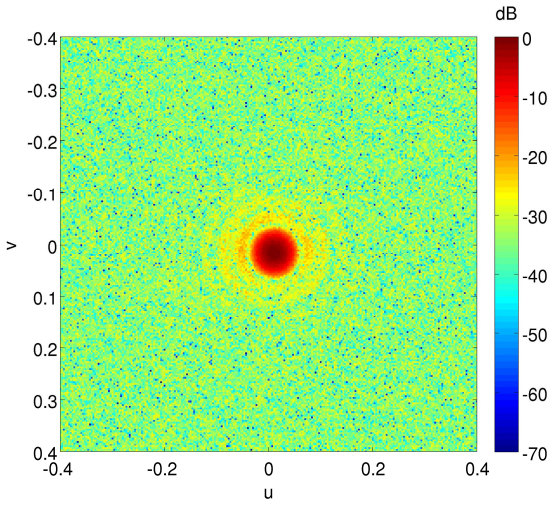


Figure 4. Amplitude (dB) of the simulated FFP corrupted by noise.

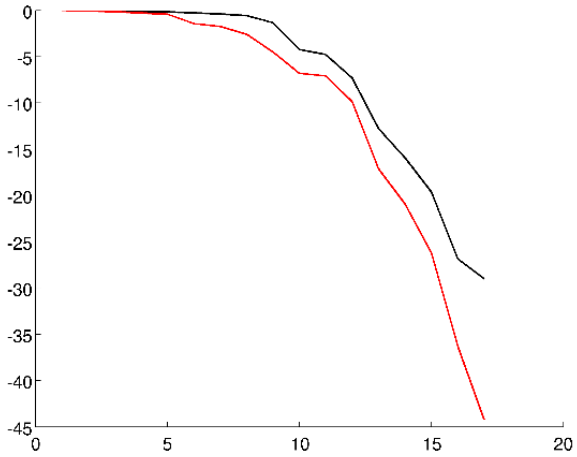


Figure 5. Normalized SVB of $\underline{\underline{T}}$. Red line: standard grid; Black line: optimal sampling points.

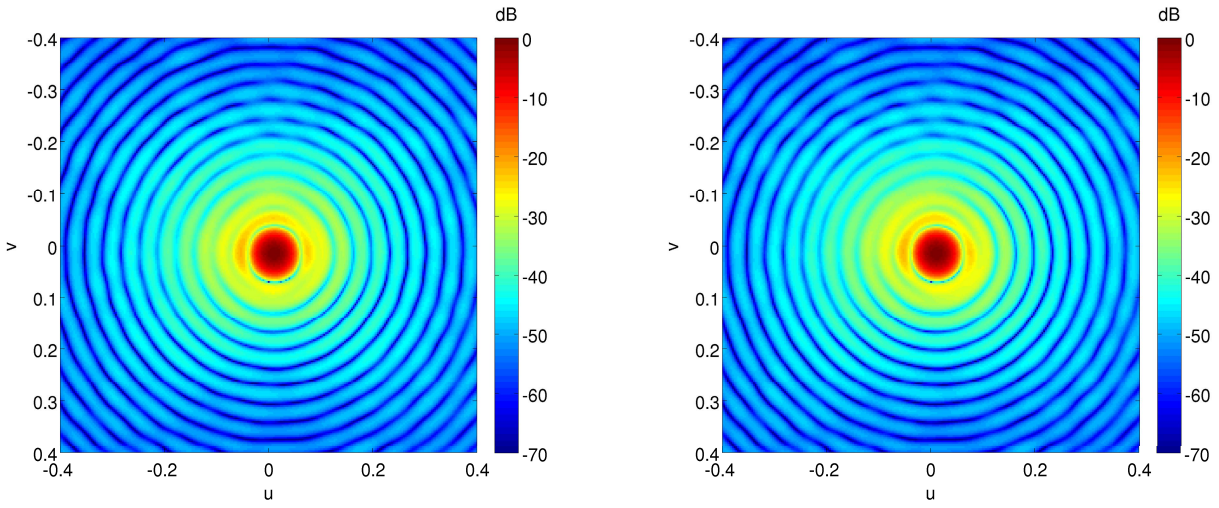


(a) (b)

Figure 6. Normalized amplitudes (dB) of the reconstructed FFP. (a): standard grid; (b): optimized grid.

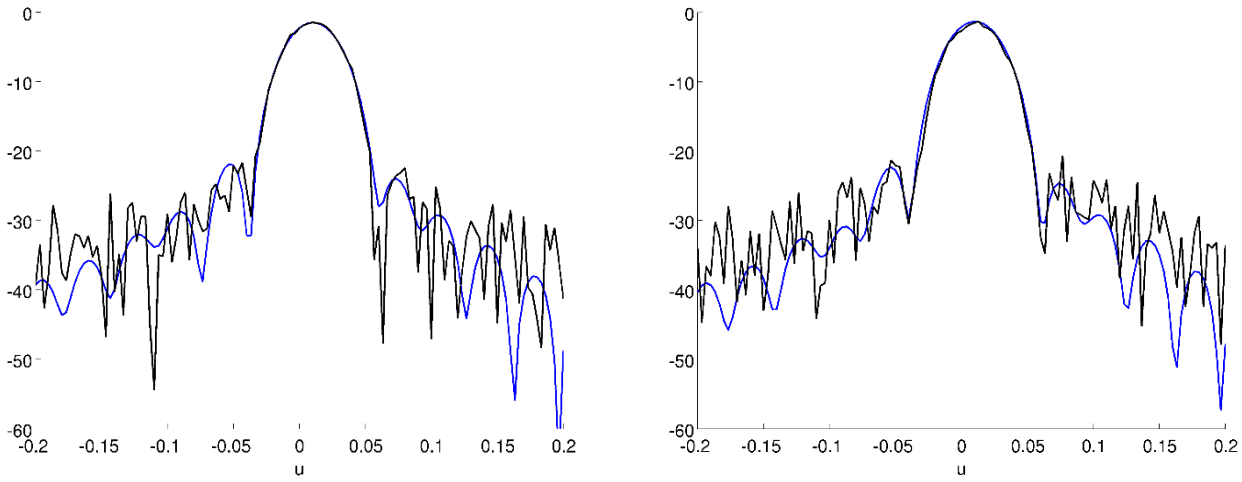


(a) (b)

Figure 7. Cut along the u-axis of the normalized amplitude (dB) of the reconstructed FFP. The black line represents the far-field data while the blue line represents the reconstructed field. (a): standard grid; (b): optimized grid.

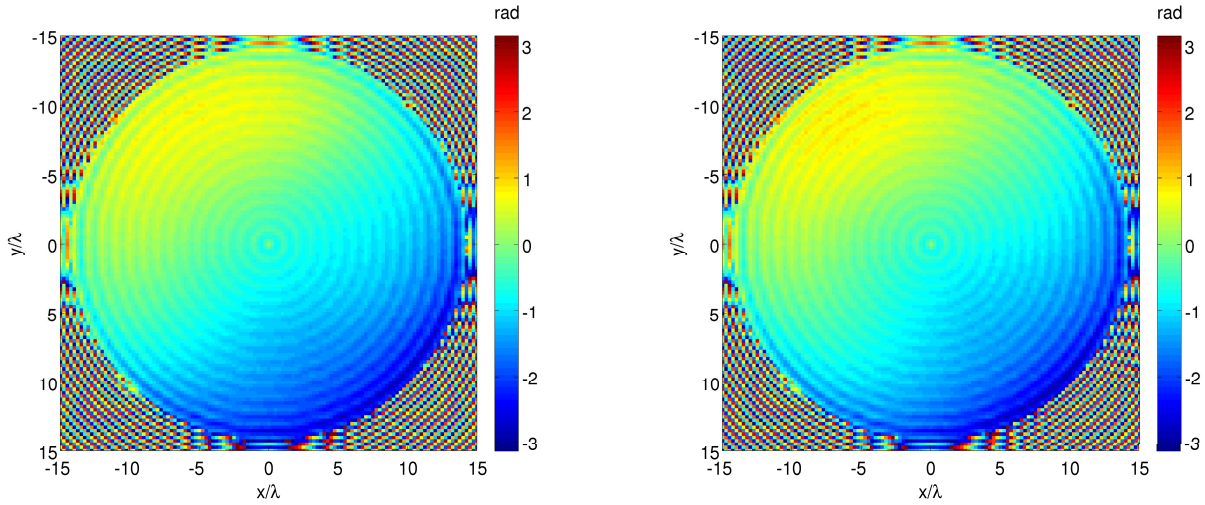


(a) (b)

Figure 8. Phase of the aberration function retrieved. (a): Standard grid; (b): Optimized grid.

## ACKNOWLEDGEMENTS

This work has been developed within an EU co-funded project - R.O.P. ERDF Campania 2007-2013 - TERA: Technologies for Radiotelescopes

## REFERENCES


[1] Rochblatt, D. J., B. L. Seidel, "Microwave Antenna Holography", IEEE Trans. on Microwave Theory and Techniques, vol. 40, n. 6, June 1992.

[2] Rajagopalan, H., Y. Rahmat-Samii, "Reflector Surface Distortion on a Sub-Reflectarray Cassegrain System: Simulations, Measurements, and Microwave Holographic Diagnostics", Proc. of the Antennas Prop. Society Int. Symp., Chicago, IL, Jul. 8-14, 1-2 (2012).

[3] Baars, J. W. M., R. Lucas, J. G. Mangum and J. A. Lopez-Perez, "Near-Field Radio Holography of Large Reflector Antennas," in IEEE Antennas and Propagation Magazine, vol. 49, no. 5, pp. 24-41, Oct. 2007.

[4] Bolli, P., G. Mazzarella, G. Montisci, and G. Serra, "An alternative solution for the reflector surface retrieval problem," Progress In Electromagnetics Research, Vol. 82, 167-188, 2008.

[5] Capozzoli, A., G. D'Elia, "Global Optimization and Antennas Synthesis and Diagnosis, Part One: Concepts, Tools, Strategies and Performances", Progr. in Electromagn. Res., Volume 56, 195-232 (2006).

[6] Capozzoli, A., G. D'Elia, "Global Optimization and Antennas Synthesis and Diagnosis, Part Two: Applications to Advanced Reflector Antennas Synthesis and Diagnosis Techniques", Progr. in Electromagn. Res., Volume 56, 233-261 (2006).

[7] Nikolic, B., R. M. Prestage, D. S. Balser, C. J. Chandler, and R. E. Hills, "Out-of-focus holography at the Green Bank Telescope", Astronomy & Astrophysics 465, no. 2, 685-693 (2007).

[8] Capozzoli, A., C. Curcio, G. D'Elia, A. Liseno, "Singular Value Optimization in Plane-Polar Near-Field Antenna Characterization", IEEE Antennas Prop. Mag., Volume 52, Issue 2, 103-112 (2010).

[9] Silver, S., Microwave Antenna Theory and Design, MIT Rad. Lab Series 12, New York, McGraw-Hill, 1949.

[10] Capozzoli, A., C. Curcio, A. Liseno, "NUFFT-Accelerated Plane-Polar (also Phaseless) Near-Field/Far-Field Transformation", Progr. in Electromagn. Res. M., Volume 27, 59-73 (2012).

[11] Capozzoli, A., C. Curcio, A. Liseno, P. Vinetti, "Field Sampling and Field Reconstruction: a New Perspective", Radio Sci., Volume 45, RS6004, 31 pp., 2010, doi:10.1029/2009RS004298.

[12] Storn, R., Price K., "Differential Evolution - A Simple and Efficient Heuristic for Global Optimization over Continuous Spaces", Journal of Global Optimization, 11, 341–359, 1997.

[13] Capozzoli, A., C. Curcio, A. Liseno, and S. Savarese, "GO solutions with Fast Marching.", 2016 10th European Conference on Antennas and Propagation (EuCAP), pp. 1 5. IEEE, 2016.

[14] Breglia, A., A. Capozzoli, C. Curcio, and A. Liseno, "Ultrafast ray tracing for electromagnetics via kD-tree and BVH on GPU.", In Applied Computational Electromagnetics (ACES), 2015 31st International Review of Progress in, pp. 1-2. IEEE, 2015.